Building homogeneous nanostructure in $Ni(OH)_2$/MWCNTs composite by electrostatic attraction

Min Shi, Yanhong Li, Hongtao Cui ✉

College of Chemistry and Chemical Engineering, Yantai University, Yantai 264005, People's Republic of China
✉ *E-mail: htcui@ytu.edu.cn*

Published in Micro & Nano Letters; Received on 15th August 2018; Revised on 14th June 2019; Accepted on 8th July 2019

A facile strategy for the preparation of composites with homogeneous distribution of multi-walled carbon nanotubes (MWCNTs) in $Ni(OH)_2$ was proposed. The electrostatic attraction between positively charged $Ni(OH)_2$ monolayer nanosheets and negatively charged MWCNTs was utilised to self-assemble the composites. The results of electrochemical measurement on the composite containing 30 wt% MWCNTs indicated that the homogeneous composition of MWCNTs in composite significantly reduced the electrical resistance and promoted the electrochemical utilisation of $Ni(OH)_2$. As a result, the composite presented high electrochemical performance: having specific capacitance of 1568.8 F g^{-1} at low current density of 2.4 A g^{-1} and keeping a relatively high specific capacitance of 781.8 F g^{-1} at high current density of 81.7 A g^{-1}. Based on the results in this works, it is hoped that the adopted strategy could provide a promising idea for the preparation of composites with homogeneous distribution of individual components.

1. Introduction: As a redox-type electrode material, $Ni(OH)_2$ is attractive for its application in supercapacitors due to its advantages of high theoretical capacity, abundant sources, low cost, and well-defined redox behaviour [1, 2]. Among the two polymorphs of layer-structured $Ni(OH)_2$ [3], α-$Ni(OH)_2$ has larger interlayer space than β-$Ni(OH)_2$, which results in its larger accessible surface for electrolyte ions. Therefore, α-$Ni(OH)_2$ could present higher capacity than β-$Ni(OH)_2$ in most cases. However, it should be noted that α-$Ni(OH)_2$ usually could not present the presumed electrochemical performance because of its low electrical conductivity that is close to insulator.

The appropriate solution of this issue is to composite $Ni(OH)_2$ homogeneously with electrically conductive materials such as graphene and carbon nanotubes (CNTs) or grow nanostructured $Ni(OH)_2$ on the surface of current collectors such as nickel foam [4–7]. CNTs is an optional material for compositing $Ni(OH)_2$ because of its outstanding electrical conductivity. An additional advantage for the usage of CNTs in the electrodes of supercapacitors is that it could efficiently buffer the cycling volume change of electroactive materials in favour of their capacitance retention [8, 9]. However, the difficulty in the homogeneous composition of CNTs with $Ni(OH)_2$ lies in the incompatibility of surface properties between the hydrophobic CNTs and hydrophilic $Ni(OH)_2$. The simple mixing of pristine CNTs with $Ni(OH)_2$ would produce inhomogeneous composites. As a result, the composites would show limited promotion of electrochemical performance [10]. The basic coping strategy is based on the transformation of CNTs' surface properties from hydrophobicity to hydrophilicity by introducing oxygenated groups [6, 11–18]. The following composition of hydrophilisation-modified CNTs with $Ni(OH)_2$ includes two strategies: (i) random mixing of modified CNTs with $Ni(OH)_2$ in aqueous suspension; (ii) growth of $Ni(OH)_2$ on the surface of CNTs forming hierarchical nanostructure. However, an issue of microscopic inhomogeneity in composites could arise from these strategies due to the lack of driving force for the ordered assembly of CNTs and $Ni(OH)_2$. In the composites prepared by the second strategy, some part of $Ni(OH)_2$ three-dimensionally grown on CNTs does not maintain intimate contact with the surface of individual CNTs. As a result, these part of $Ni(OH)_2$ would not attribute significant capacitance to supercapacitors due to its low electrical conductivity.

In this work, we adopted an effective chemical synthetic strategy to build $Ni(OH)_2$/CNTs composites with intimate contact between individual components. During the synthesis, we utilised the electrostatic attraction between the positively charged α-$Ni(OH)_2$ monolayer nanosheets and negatively charged CNTs. Due to the intimate contact between components, the as-prepared composite presented significant synergy effect on its electrochemical performance.

2. Experimental: Multi-walled CNTs (MWCNTs, 40–60 nm, ≥97%) were purchased from Shenzhen Nanotech Port Co. Nitric acid (HNO_3, 65.0–68.0%), ethanol (C_2H_5OH, ≥99.0%), nickel nitrate hexahydrate ($Ni(NO_3)_2{\cdot}6H_2O$, ≥98.0%), formamide (CH_3NO, ≥99.5%), and morpholine (C_4H_9NO, ≥98.5%) were purchased from Aladdin. All raw materials were used as received.

Modification of MWCNTs: 0.5 g MWCNTs were modified by 50 ml nitric acid at 140 °C for 1 h. The obtained suspension was mixed with 1 l distilled water. Then, the modified MWCNTs was separated from the suspension by vacuum filtration and washed with distilled water. In the final step, the separated MWCNTs were freeze-dried.

Synthesis of α-$Ni(OH)_2$ monolayer nanosheets: The α-$Ni(OH)_2$ monolayer nanosheets were prepared using exactly the same method used in our previous work [19] as shown in the following procedure. A mixture of 0.5 g $Ni(NO_3)_2{\cdot}6H_2O$ and 1 ml morpholine was ground at room temperature in a mortar for 5 min. The obtained sticky paste was aged for 4 h at room temperature. Then, the aged paste was dispersed in 25 ml formamide under ultrasonification for 5 min, forming a transparent colloidal solution.

Synthesis of $Ni(OH)_2$/MWCNTs composites: 15.0 mg modified MWCNTs were dispersed in 100 ml distilled water under ultrasonification for 1 h, forming a brownish colloidal solution. Then, several colloidal solutions of modified MWCNTs were, respectively, mixed with different amount of α-$Ni(OH)_2$ colloidal solutions. Precipitation occurred immediately after the mixing of colloidal solutions. The precipitate was separated from the produced suspension by vacuum filtration, and then washed with distilled water and freeze-dried.

Characterisation: The structure of composites was measured with a Rigaku SmartLab III diffractometer using Cu Kα radiation ($\lambda = 1.5406$ Å). The Micro-Raman spectroscopy of samples was measured by Fuheng K-Sens Raman spectrometer. JEOL JEM-1400 transmission electron microscope (TEM) and Hitachi S-4800 cold-cathode field-emission scanning electron microscope (FE-SEM) were used to observe the morphology of samples. The elemental analysis on the samples was carried out with a Bruker XFlash 6|60 detector. The TEM sample of α-$Ni(OH)_2$ was prepared by the following procedure: 0.5 ml α-$Ni(OH)_2$ colloidal solution was mixed with 5 ml formamide; then, the α-$Ni(OH)_2$ monolayer nanosheets were deposited on the surface of a 400-mesh carbon-coated copper grid for 15 s; in the next step, the α-$Ni(OH)_2$-deposited copper grid was washed with ethanol to remove the residual formamide. The SEM samples were prepared by the deposition of gold nanoparticles on the surface of materials with an ion sputtering method.

An IVIUMSTAT electrochemical workstation in a three-electrode cell having a working electrode, a platinum plate counter electrode, and a Hg/HgO reference electrode was used to carry out the electrochemical measurements on electrode materials.

Preparation of working electrodes and electrochemical measurement: The working electrodes for electrochemical measurement were assembled by the combination of electro-active material with nickel foam. In the first step, a paste was formed by grinding a mixture of 80 wt% MWCNTs/$Ni(OH)_2$ composite and 20 wt% acetylene black with a few drops of ethanol. In the second step, a working electrode containing ~4 mg electro-active material and having 1 cm^2 geometric surface area was obtained by the brief evaporation of ethanol in paste and the following compression of paste at 10 MPa onto a nickel foam connected with a nickel wire. Then, the electrode was electro-activated by 100 cycles of cyclic voltammetry from −0.1 to 0.55 V versus Hg/HgO at 100 mV s^{-1} in 3 M KOH aqueous solution. All electrochemical tests on the activated electrodes were performed in 3 M KOH aqueous solution. The specific capacitance calculation of electro-active material was based on the method described in literature [20] using the weight of composites as basis.

3. Results and discussion: In this work, the α-$Ni(OH)_2$ monolayer nanosheets were prepared by exactly the same method used in our previously published articles [19, 21]. In these articles, the monolayer state of α-$Ni(OH)_2$ was confirmed by atomic force microscopy and TEM characterisations. Herein, we repeated the XRD and TEM characterisations to show the phase and morphology of α-$Ni(OH)_2$ monolayer. The XRD pattern shown in Fig. 1*a* proves that the as-prepared sample does present the typical rhombothedral structure of α-$Ni(OH)_2$ (JCPDS Card No. 38-0715). In this pattern, the great broadening and low intensity of diffraction lines implies the characteristics of thin thickness and low crystallinity of α-$Ni(OH)_2$ sample. The TEM images at different magnification shown in Figs. 1*b–d* also demonstrate the monolayer and low crystallinity state of α-$Ni(OH)_2$ sample. In these images, it is observed that the carbon-coated copper grid is covered by some fragmental sheet-like subjects with hardly distinguishable boundary. It is considered that this morphology of α-$Ni(OH)_2$ corresponds to its low crystallinity characteristics as observed in XRD pattern.

In this work, we composited the as-prepared α-$Ni(OH)_2$ with MWCNTs trying to improve the electrical conductivity of α-$Ni(OH)_2$. To determine the optimum content of MWCNTs in the composites, we composited α-$Ni(OH)_2$ with different amount of modified MWCNTs and investigated their electrochemical performance. The specific capacitance of composites is shown in Fig. 2*a*, which is calculated on the basis of the composites' weight. This figure indicates that the composite containing 30 wt % MWCNTs has the largest capacitance at high current density, while the medium capacitance at low current density as compared with other composites. Based on this result, we chose 30 wt% as the optimum content of MWCNTs in the composites.

To investigate the effect of surface modification for MWCNTs on the performance of composites, we also prepared the $Ni(OH)_2$/MWCNTs composites using pristine MWCNTs by the same procedure with the composites prepared by using modified MWCNTs. As shown in Fig. 2*b*, the composites containing different amount of pristine MWCNTs exhibit comparable

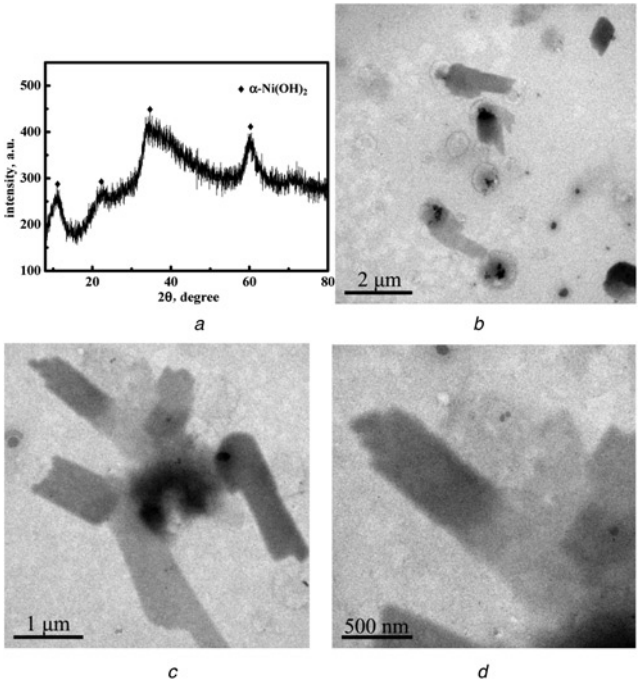

Fig. 1 *XRD pattern and TEM images of α-$Ni(OH)_2$ monolayer nanosheets at different magnification*
a XRD pattern
b–d TEM images

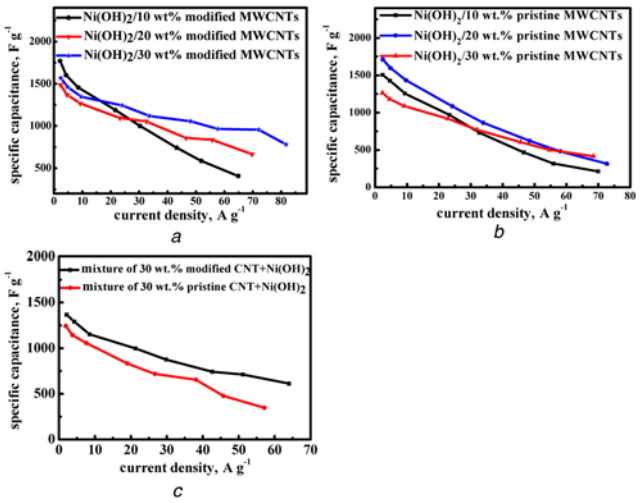

Fig. 2 *Specific capacitance of the composites containing different amount of*
a Modified MWCNTs
b Pristine MWCNTs, calculated from their galvanostatic charge–discharge plots
c Specific capacitance of the mixture composites prepared by the respective grinding of modified and pristine MWCNTs with $Ni(OH)_2$, calculated from their galvanostatic charge–discharge plots

doi: 10.1049/mnl.2018.5469

electrochemical performance. For the aim of a fair comparison, we choose the composite containing 30 wt% pristine MWCNTs for further investigation. We also prepared other two mixture composites by the respective grinding of pristine and modified MWCNTs with $Ni(OH)_2$ powder in a mortar. In Fig. 2*c*, the two mixture composites show much lower specific capacitance as compared with their corresponding composites prepared by the strategy of solution deposition (Fig. 2), especially at high current density. Obviously, the low performance of these two mixture composites could be attributed to the low homogeneity of MWCNTs inside composites. To keep the conciseness of this Letter, we would not discuss the two composites in the following text.

The electrochemical properties of the two composites, respectively, prepared by the strategy of solution deposition using pristine and modified MWCNTs are compared with the $Ni(OH)_2$ sample in Fig. 3. In the cyclic voltammogram (CV) at scan rate of 5 mV s^{-1} (Fig. 3*a*), all the three samples have a pair of symmetrical redox peaks, corresponding to the reversible Faradaic reactions of $Ni(OH)_2 \leftrightarrow NiOOH$ as shown in (1) [22]. The symmetrical non-linear shape of glavanostatic charge–discharge plots of these samples (Fig. 3*b*) is another indication of Faradaic reactions. These plots also show that the $Ni(OH)_2$ sample has the longest charge–discharge cycle duration at low current density of ~2.5 A g^{-1}, while the composite containing 30 wt% modified MWCNTs present the longest cycle duration at high current density of 57.5 A g^{-1}. This result suggests that this composite has the best high-rate electrochemical performance among these three samples. In Fig. 3*c*, the plots of specific capacitance versus specific capacitance confirm this conclusion. The composite containing 30 wt% modified MWCNTs has specific capacitance of 1568.8 F g^{-1} at 2.4 A g^{-1} and keeps relatively high capacity of 781.8 F g^{-1} at high current density of 81.7 A g^{-1}. Although the $Ni(OH)_2$ sample has the highest capacity of 1933.9 F g^{-1} at low current density of 2.4 A g^{-1}, it should be pointed out that the capacity calculation on the two composites is based on the weight of composites including MWCNTs and $Ni(OH)_2$. To consider the contribution of MWCNTs, we recalculated the capacity of the two composites using the weight of $Ni(OH)_2$ as a basis for the calculation. As shown in the result (Fig. 3*d*), the composite containing 30 wt% modified MWCNTs presents the much higher capacity

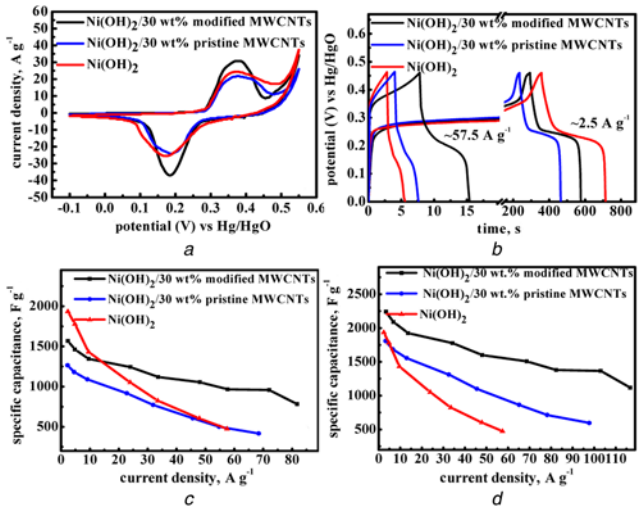

Fig. 3 *CV of composites and Ni(OH)₂ at*
a Scan rate of 5 mV s^{-1}
b Glavanostatic charge–discharge plots of composites and $Ni(OH)_2$ at current density of ~2.5 A g^{-1}
c Specific capacitance of composites and $Ni(OH)_2$ calculated from their galvanostatic charge–discharge plots
d Specific capacitance of composites and $Ni(OH)_2$ calculated from their corresponding galvanostatic charge–discharge curves

than the other two samples. It has high specific capacitance of 2241.0 F g^{-1} at low current density 3.3 A g^{-1} and 1116.8 F g^{-1} at high current density of 116.8 A g^{-1}

$$Ni(OH)_2 + OH^- \leftrightarrow NiOOH + H_2O + e^- \quad (1)$$

In order to clarify the role of MWCNTs in the performance of composites, we measured the electrochemical impedance spectroscopy (EIS) of composites and $Ni(OH)_2$. Their Nyquist plots (Fig. 4) are analysed from the obtained EIS and fitted with the given equivalent circuit by software ZVIEW. In the plots, the two composites, respectively, prepared from the modified and pristine MWCNTs exhibit similar impedance behaviour, which is completely different from the $Ni(OH)_2$ sample. The $Ni(OH)_2$ sample presents a more intensive semicircle with large diameter in high-frequency region related with charge transfer resistance, and smaller slop of line in low-frequency region related with ions transfer resistance than the two composites. It could be inferred from these impedance results that the two composites have low resistance for the Faradaic reactions, which could be attributed to MWCNTs.

As proven in electrochemical measurement, the composition of MWCNTs with $Ni(OH)_2$ contributes to the promotion of electrochemical performance. It could be imagined that the composition homogeneity of MWCNTs is the control for the electrochemical performance of composites. To support this opinion, we used FE-SEM to observe the morphology of composites. As shown in the FE-SEM image of the composite containing 30 wt% pristine MWCNTs at low magnification (Fig. 5*a*), the MWCNTs inhomogeneously distribute inside $Ni(OH)_2$. In the images at high magnification (Figs. 5*b* and *c*), it seems that no $Ni(OH)_2$ in the MWCNTs-concentrated part of composite could be observed. By contrast, the FE-SEM images of the composite containing 30 wt% modified MWCNTs present homogeneous distribution of MWCNTs. In the image at low magnification (Fig. 5*d*), it seems that the MWCNTs homogeneously distribute in $Ni(OH)_2$. The images at high magnification (Figs. 5*e* and *f*) clearly indicate that the surface of modified MWCNTs is much rougher than the pristine MWCNTs and no separate $Ni(OH)_2$ can be observed. It could be inferred from the morphology observation that the surface of MWCNTs is coated by $Ni(OH)_2$, having a coaxial core–shell nanostructure similar with other works [23, 24].

To further confirm the homogeneity of MWCNTs in $Ni(OH)_2$, the elemental mapping characterisation was carried out on the two composites. In the obtained mapping images (Fig. 6), it is shown that only small amount of nickel (0.57%) and oxygen (3.83%) elements are detected in the composite containing 30 wt% pristine MWCNTs, while much larger amount of nickel (4.17%) and oxygen (12.12%) elements are found in the composite containing 30 wt% modified MWCNTs. It is also observed that the nickel and oxygen elements are homogeneously distributed in the latter composite. The over high content of carbon element (95.60 and 83.71%) in the two composites could be attributed to

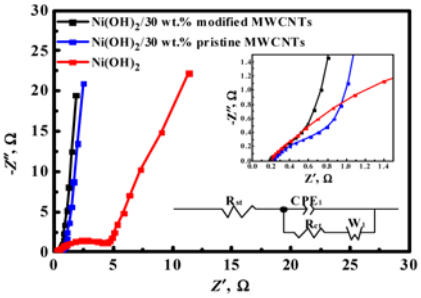

Fig. 4 *Nyquist plots of composites and Ni(OH)₂*

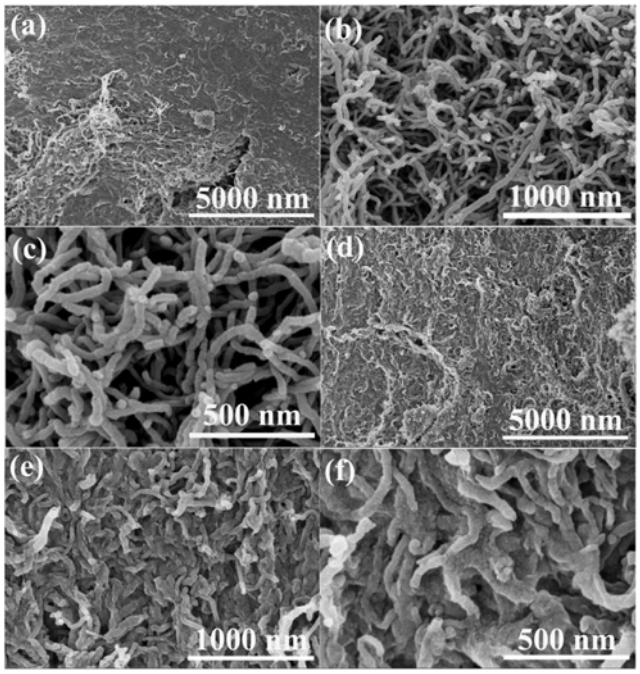

Fig. 5 *FE-SEM images of the composites, respectively, prepared by using*
a–c 30 wt% pristine
d–f 30 wt% modified MWCNTs

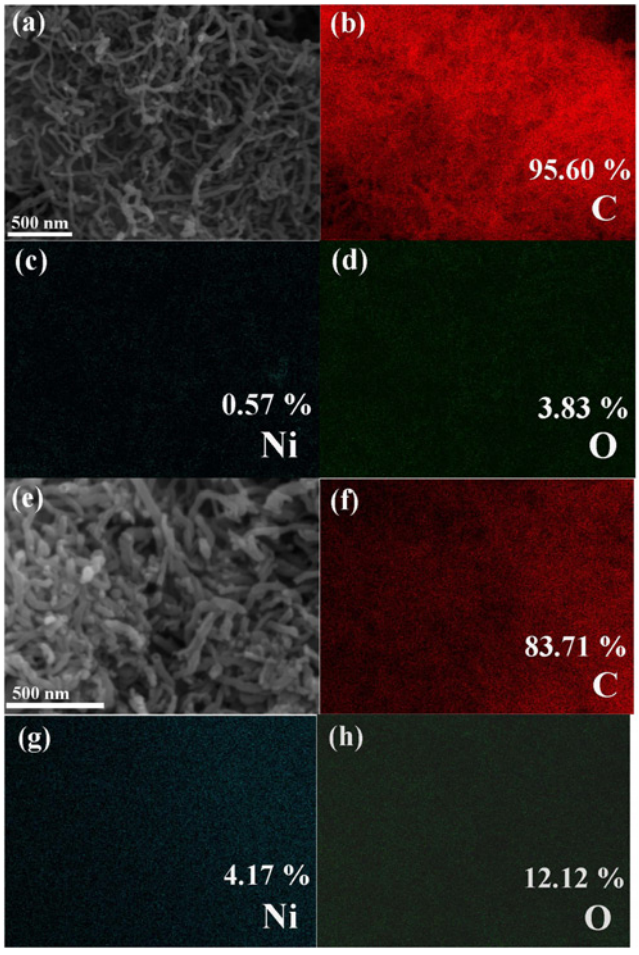

Fig. 6 *Elemental mapping of the composites, respectively, prepared by using*
a–d 30 wt% pristine
e–h 30 wt% modified MWCNTs

the contribution of conductive tape used for the FE-SEM characterisation. Herein, it could be concluded that the elemental mapping result agrees with the morphology observation result in Fig. 5.

We also measured the Micro-Raman spectra of pristine MWCNTs, modified MWCNTs and their $Ni(OH)_2$ composites. As shown in Fig. 7, all samples present the characteristic feature of graphitic layers corresponding to the tangential vibration of carbon atoms (G band) and the typical sign of defective graphitic structures (D band). It is well known that the G band represents the in-plane bond stretching motion of the pairs of C sp^2 atoms and the D band corresponds to the sp^3 hybridisation of C atoms. Thus, the relative intensity of G and D bands (I_D/I_G) is considered as a measure for the surface defects of graphitic materials [25, 26]. As a result, the nearly same I_D/I_G value (~1) for the pristine and modified MWCNTs in this work indicates that the modification by nitric acid could not significantly influence the surface state of MWCNTs. In some works [27–29], it was reported that the combination of $Ni(OH)_2$ and carbon materials would result in the increase of surface defects in carbon materials. Therefore, it is reasonable to believe that the lowered I_D/I_G value of composites in this work (0.93 for 30 wt% pristine MWCNTs composited $Ni(OH)_2$ and 0.85 for 30 wt% modified MWCNTs composited $Ni(OH)_2$) is ascribed to the homogeneous composition of MWCNTs with $Ni(OH)_2$. On the other hand, the lower I_D/I_G value for the latter composite could confirm its higher homogeneity of $Ni(OH)_2$. Based on the results of FE-SEM and Raman spectra, we know that the performance difference between the two composite originates from their different homogeneity of MWCNTs.

It is known that the capacitance decay of electrode materials during the cycle of charge–discharge is mainly because of their redox reaction-induced volume contract and expansion. Therefore, one important function of MWCNTs in this work is to work as supporting network to buffer the electrochemical volume change of electrode materials. We compared the cycle stability of $Ni(OH)_2$ with the composite containing 30 wt% modified MWCNTs. As shown in Fig. 8, the specific capacitance of $Ni(OH)_2$ decreases

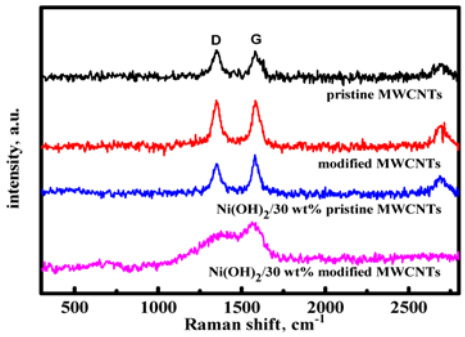

Fig. 7 *Micro-Raman spectra of pristine MWCNTs, modified MWCNTs, and composites prepared by using 30 wt% pristine or modified MWCNTs*

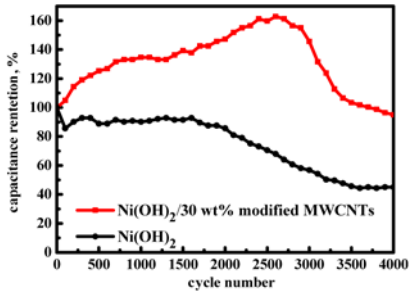

Fig. 8 *Stability of cycle of the composite prepared by using 30 wt% modified MWCNTs at charge–discharge current density of ~2.4 A* g^{-1}

doi: 10.1049/mnl.2018.5469

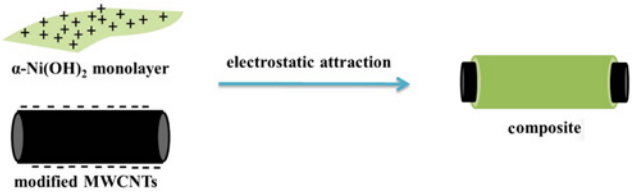

Fig. 9 *Schematic illustration for the preparation of $Ni(OH)_2$/MWCNTs composites using modified MWCNTs*

gradually with the charge–discharge cycles, keeping 45% of its initial value after 4000 cycles. On the contrary, it is surprising to notice that the specific capacitance of composite increases gradually with the charge–discharge cycles, reaching the highest value (162% of initial value) at 2600 cycles. This phenomenon could be attributed to the continuous electro-activation of $Ni(OH)_2$ in the composite due to the promotion of electrochemical utilisation rate for $Ni(OH)_2$ by rising its electrical conductivity with MWCNTs. After 4000 cycles, the specific capacitance of composite still remains 95% of its initial value, much higher than $Ni(OH)_2$.

In Fig. 9, we provide a schematic illustration for the preparation of composite with homogeneous distribution of MWCNTs. It is well known that the surface of pristine MWCNTs is hydrophobic. Therefore, the simple mixing of pristine MWCNTs with hydrophilic $Ni(OH)_2$ would only result in the random distribution of MWCNTs inside $Ni(OH)_2$. The surface modification of pristine MWCNTs by nitric acid would produce carboxyl groups, introducing the hydrophilic property and negative charge on their surface [8, 30]. On the other hand, the α-$Ni(OH)_2$ monolayer nanosheets are positively charged due to the non-stoichiometry characteristics of $Ni(OH)_{2-x}$ layer [31]. As a result, the mixing of the α-$Ni(OH)_2$ and MWCNTs colloidal solution would result in the formation of homogeneous $Ni(OH)_2$ /MWCNTs composites due to the spontaneous electrostatic attraction between the two species.

As shown in the Nyquist plots of Fig. 4, the homogeneous composition of $Ni(OH)_2$ and modified MWCNTs results in the significant lowering of resistance. As a result, the charge transfer resistance of $Ni(OH)_2$ is reduced. On the other hand, the isolated state of $Ni(OH)_2$ originating from the homogeneous composition with MWCNTs is in favour of the transfer of electrolyte ions inside composites, which can be proven by the larger slop in low-frequency region in Fig. 4. Consequently, the $Ni(OH)_2$/MWCNTs composites could present promoted performance.

4 Conclusions: In this work, a simple method was applied to synthesise $Ni(OH)_2$/MWCNTs composite to solve the poor conductivity issue of $Ni(OH)_2$ in order to obtain electrode materials having high electrochemical performance. The composite with homogeneous distribution of MWCNTs was obtained by the self-assembly of MWCNTs and $Ni(OH)_2$ through the spontaneous electrostatic attraction between the two oppositely charged species. Due to the high homogeneity of MWCNTs inside $Ni(OH)_2$, the composite presented significant promotion of electrochemical performance.

5 References

[1] Kim S.W., Kim I.H., Kim S.I., *ET AL.*: 'Nickel hydroxide supercapacitor with a theoretical capacitance and high rate capability based on hollow dendritic 3D-nickel current collectors', *Chem-Asian J.*, 2017, **12**, (12), pp. 1291–1296

[2] Li B., Zheng M., Xue H., *ET AL.*: 'High performance electrochemical capacitor materials focusing on nickel based materials', *Inorg. Chem. Front.*, 2016, **3**, (2), pp. 175–202

[3] Hall D.S., Lockwood D.J., Bock C., *ET AL.*: 'Nickel hydroxides and related materials: a review of their structures, synthesis and properties', *Proc. R. Soc. A*, 2015, **471**, p. 20140792

[4] Sun Z., Lu X.: 'A solid-state reaction route to anchoring $Ni(OH)_2$ nanoparticles on reduced graphene oxide sheets for supercapacitors', *Ind. Eng. Chem. Res.*, 2012, **51**, (30), pp. 9973–9979

[5] Zhang J.T., Liu S., Pan G.L., *ET AL.*: 'A 3D hierarchical porous α–$Ni(OH)_2$/graphite nanosheet composite as an electrode material for supercapacitors', *J. Mater. Chem. A*, 2014, **2**, (5), pp. 1524–1529

[6] Wang B., Williams G.R., Chang Z., *ET AL.*: 'Hierarchical NiAl layered double hydroxide/multiwalled carbon nanotube/nickel foam electrodes with excellent pseudocapacitive properties', *ACS Appl. Mater. Interfaces*, 2014, **6**, (18), pp. 16304–16311

[7] Wang L., Li X., Guo T., *ET AL.*: 'Three-dimensional $Ni(OH)_2$ nanoflakes/graphene/nickel foam electrode with high rate capability for supercapacitor applications', *Int. J. Hydrogen Energy*, 2014, **39**, (15), pp. 7876–7884

[8] Chinnappan A., Baskar C., Kim H., *ET AL.*: 'Carbon nanotube hybrid nanostructures: future generation conducting materials', *J. Mater. Chem. A*, 2016, **4**, (24), pp. 9347–9361

[9] Karousis N., Tagmatarchis N., Tasis D.: 'Current progress on the chemical modification of carbon nanotubes', *Chem. Rev.*, 2010, **110**, (9), pp. 5366–5397

[10] Wang X., Ruan D., You Z.: 'Application of spherical $Ni(OH)_2$/CNTs composite electrode in asymmetric supercapacitor', *Trans. Nonferr. Met. Soc. China*, 2006, **16**, (5), pp. 1129–1134

[11] Zhang L., Chen R., Hui K.N., *ET AL.*: 'Hierarchical ultrathin NiAl layered double hydroxide nanosheet arrays on carbon nanotube paper as advanced hybrid electrode for high performance hybrid capacitors', *Chem. Eng. J.*, 2017, **325**, pp. 554–563

[12] Fan J., Mi H., Xu Y., *ET AL.*: 'In situ fabrication of $Ni(OH)_2$ nanofibers on polypyrrole-based carbon nanotubes for high-capacitance supercapacitors', *Mater. Res. Bull.*, 2013, **48**, (3), pp. 1342–1345

[13] Ma X., Li Y., Wen Z., *ET AL.*: 'Ultrathin beta-$Ni(OH)_2$ nanoplates vertically grown on nickel-coated carbon nanotubes as high-performance pseudocapacitor electrode materials', *ACS Appl. Mater. Interfaces*, 2015, **7**, (1), pp. 974–979

[14] Wu Q., Wen M., Chen S., *ET AL.*: 'Lamellar-crossing-structured $Ni(OH)_2$ /CNTs/$Ni(OH)_2$ nanocomposite for electrochemical supercapacitor materials', *J. Alloys Compd.*, 2015, **646**, pp. 990–997

[15] Yi H., Wang H., Jing Y., *ET AL.*: 'Advanced asymmetric supercapacitors based on CNT@$Ni(OH)_2$ core–shell composites and 3D graphene networks', *J. Mater. Chem. A*, 2015, **3**, (38), pp. 19545–19555

[16] Salunkhe R.R., Lin J., Malgras V., *ET AL.*: 'Large-scale synthesis of coaxial carbon nanotube/$Ni(OH)_2$ composites for asymmetric supercapacitor application', *Nano Energy*, 2015, **11**, pp. 211–218

[17] Dubal D.P., Gund G.S., Lokhande C.D., *ET AL.*: 'Decoration of spongelike $Ni(OH)_2$ nanoparticles onto MWCNTs using an easily manipulated chemical protocol for supercapacitors', *ACS Appl. Mater. Interfaces*, 2013, **5**, (7), pp. 2446–2454

[18] Wu M.S., Zheng Z.B., Lai Y.S., *ET AL.*: 'Nickel cobaltite nanograss grown around porous carbon nanotube-wrapped stainless steel wire mesh as a flexible electrode for high-performance supercapacitor application', *Electrochim. Acta*, 2015, **182**, pp. 31–38

[19] Ma W., Wang L., Li Y., *ET AL.*: 'Synthesis of periodically stacked 2D composite of α-$Ni(OH)_2$ monolayer and reduced graphene oxide as electrode material for high performance supercapacitor', *Adv. Powder Technol.*, 2018, **29**, (3), pp. 631–638

[20] Lee J.W., Ko J.M., Kim J.D.: 'Hierarchical microspheres based on α-$Ni(OH)_2$ nanosheets intercalated with different anions: synthesis, anion exchange, and effect of intercalated anions on electrochemical capacitance', *J. Phys. Chem. C*, 2011, **115**, (39), pp. 19445–19454

[21] Ma W., Wang L., Xue J., *ET AL.*: 'Ultra-large scale synthesis of Co-Ni layered double hydroxides monolayer nanosheets by a solvent-free bottom-up strategy', *J. Alloys Compd.*, 2016, **662**, pp. 315–319

[22] Yang G.W., Xu C.L., Li H.L.: 'Electrodeposited nickel hydroxide on nickel foam with ultrahigh capacitance', *Chem. Commun.*, 2008, **48**, pp. 6537–6539

[23] Li M., Ma K.Y., Cheng J.P., *ET AL.*: 'Nickel–cobalt hydroxide nanoflakes conformal coating on carbon nanotubes as a supercapacitive material with high-rate capability', *J. Power Sources*, 2015, **286**, pp. 438–444

[24] Zhao J., Chen J., Xu S., *ET AL.*: 'Hierarchical NiMn layered double hydroxide/carbon nanotubes architecture with superb energy density for flexible supercapacitors', *Adv. Funct. Mater.*, 2014, **24**, (20), pp. 2938–2946

[25] Costa S., Borowiak-Palen E., Kruszyńska M., *ET AL.*: 'Characterization of carbon nanotubes by Raman spectroscopy', *Mater. Sci. (Poland)*, 2008, **26**, (2), pp. 433–441

[26] Dresselhaus M.S., Dresselhaus G., Saito R., *ET AL.*: 'Raman spectroscopy of carbon nanotubes', *Phys. Rep.*, 2005, **409**, (2), pp. 47–99
[27] Yan H., Bai J., Wang J., *ET AL.*: 'Graphene homogeneously anchored with $Ni(OH)_2$ nanoparticles as advanced supercapacitor electrodes', *CrystEngComm*, 2013, **15**, (46), pp. 10007–10015
[28] Yan J., Sun W., Wei T., *ET AL.*: 'Fabrication and electrochemical performances of hierarchical porous $Ni(OH)_2$ nanoflakes anchored on graphene sheets', *J. Mater. Chem.*, 2012, **22**, (23), pp. 11494–11502
[29] Cho E.C., Chang-Jian C.W., Lee K.C., *ET AL.*: 'Ternary composite based on homogeneous $Ni(OH)_2$ on graphene with Ag nanoparticles as nanospacers for efficient supercapacitor', *Chem. Eng. J.*, 2018, **334**, pp. 2058–2067
[30] Lee S.W., Kim B.S., Chen S., *ET AL.*: 'Layer-by-layer assembly of all carbon nanotube ultrathin films for electrochemical applications', *J. Am. Chem. Soc.*, 2009, **131**, (2), pp. 671–679
[31] Schneiderová B., Demel J., Pleštil J., *ET AL.*: Nickel hydroxide ultrathin nanosheets as building blocks for electrochemically active layers', *J. Mater. Chem. A*, 2013, **1**, (37), pp. 11429–11437

doi: 10.1049/mnl.2018.5469